SUPPLEMENTARY DATA

Method S1. Estimation of the ratio between the final length of internode *n* and sheath *n*–1

To estimate the final length of internode *n*, a relationship between the final length of internode *n* and the final length of the encapsulating sheath (*n*–1) was set up. The ratio between final length of internode *n* and sheath *n*–1 was fitted according to a quadratic function (Eq. S1). Regressions were made using the nonlinear least square function (nls) in the 'stats' package of the R programming language (R Development Core Team, 2012).

Complementary data of normal density 'Déa' in 1996, and 'Nobilis' in 1998 and in 2000 were also used for quantifying the relationship between final length of internode *n* and final length of the encapsuling sheath (*n*-1). The agronomic treatments and data collection in these experiments were similar as in the experiment with Déa in 2000. Relative rank, defined as the ratio between current rank and final rank, was used since the final leaf number for normal density 'Déa' in 1996 was 17 while all others were 15.

$$ratio_{int/sth} = ratio_{max} * \left(2 * \rho_{max} - \rho_b - \rho\right) * \frac{\left(\rho - \rho_b\right)}{\left(\rho_{max} - \rho_b\right) \wedge 2} \qquad \text{(Eq. S1)}$$

where $ratio_{int/sth}$ is the ratio between final length of internode *n* and sheath *n-1*, $ratio_{max}$ is the maximum ratio, ρ_{max} is the relative phytomer rank where maximum ratio is reached, ρ_b is the relative starting rank where the $ratio_{int/sth}$ is equal to zero. For model implementation, final leaf number was fixed to 15 and relative ranks was transferred to real ranks. The fitted $ratio_{max}$ was 1.29 ± 0.2, ρ_{max} was 0.78 ± 0.03, ρ_b was 0.24 ± 0.02. The fitting results were shown in Fig. S2.

Method S2. Justification of coordination rules used in the model

The model is based on a detailed consideration of empirical data and proposed mechanisms for coordination of leaf growth in maize and other species in the Poaceae. Here we summarize the main empirical findings supporting our model.

Dynamics of blade extension

- Blade initiation occurs at a constant thermal time interval. The initiation of a blade is defined as the moment when the length of the blade reaches 0.25 mm (Andrieu et al., 2006).
- The linear phase of blade growth was found to start close to the time of leaf tip emergence for blades of ranks below 10, and before that for higher ranks (Andrieu *et al.*, 2006), which supports the notion that the exponential phase of growth ends at tip emergence.
- Several studies found that the rate of cell division in the blade declined rapidly after tip emergence (Wilson and Laidlaw, 1985; Casey *et al.*, 1999; Parent *et al.*, 2009).
- The growing zone is shorter than the sheath tube and in the exposed section of a leaf, both cell division and cell enlargement have ceased (Begg and Wright, 1962; Davidson and Milthorpe, 1966).

- The extension of the blade and sheath are highly coordinated (Schnyder *et al.*, 1990; Casey *et al.*, 1999; Parent *et al.*, 2009). Once the ligule is differentiated, it propagates passively within the growing zone, delimiting an increasing sheath growing zone (basal) and a decreasing blade growing zone (apical) (Skinner and Nelson, 1994).

Dynamics of sheath extension: The extension of the sheath contains three growth phases in this model: an exponential phase, a linear phase, and a decline phase. We distinguish events occurring before and after the switch to the generative phase, i.e. the initiation of the tassel, for sheath dynamics.

Before tassel initiation:

- In maize and rice (*Oryza spp*), sheath initiation (observable at a minimum length of 1 to 3 mm) was found to occur simultaneously with tip emergence of the same leaf (Andrieu *et al.*, 2006; Parent *et al.*, 2009).
- The dynamics of sheath extension was described by a model possessing exponential plus linear growth phases (Hillier *et al.*, 2005).
- For phytomers below rank 8, the change to the linear phase of extension took place later (in both time and length) in higher density than in normal density (Andrieu *et al.*, 2006).
- The decline of sheath elongation rate was synchronized with the emergence of the collar of the phytomer in question (Fournier and Andrieu, 2000a).

After tassel initiation:

- Two features have been identified for sheath initiation shortly after tassel initiation (Paysant-Leroux, 1998; Andrieu et al., 2006): (a) Collars became distinguishable on several leaves within a short period of time, although the corresponding sheaths had different lengths. (b) After this short period, the rate of emergence of distinguishable collars on leaves at higher ranks was close to that of leaf initiation.
- For phytomers 8-10, early sheath development was delayed in high density compared with normal density but fast extension took place simultaneously in both treatments (Andrieu et al., 2006).
- For phytomers 11 and above, the dynamics of sheath extension were identical in both low and high population density from the first date of accurate measurement up to a size of 5-8 cm, after which sheath expansion took place at a lower rate in the high density treatment (Andrieu et al., 2006).

Dynamics of internode extension: The extension of the internode contains three phases in this model: an exponential phase, a transition phase, and a linear phase.

- Internodes are initiated having one single cell layer (20 µm), at about half a plastochron after the initiation of the corresponding leaf primordium (Sharman, 1942; Fournier and Andrieu, 2000a).
- Internodes elongate exponentially until the collar emergences of the phytomer in question.
- After collar emergence, the elongation rate of the sheath declines and the elongation rate of the internode increases rapidly, while their sum was close to the linear elongation rate of the internode for both full light and shade conditions (Fournier and Andrieu, 2000b; Fournier and Andrieu, 2000a). However, such rapid elongation rate increase can only be found from ear initiation onwards defined as the time of lengthening of the axillary meristem (Siemer et al., 1969; Kiesselbach, 1999).

Method S3. Calculation of decline coefficient (d) of the elongation rate of sheath

$$\begin{cases} \dfrac{dE_n}{dt} = \dfrac{dS_n}{dt} + \dfrac{dI_n}{dt} \\ \dfrac{dS_n}{dt} = \dfrac{dS_n}{dt} - d * E_n \end{cases} \qquad \text{(Eq. S2)}$$

Where S_n is the length of sheath n (cm) and I_n is the length of internode n. E_n is the sheath length that out of the sheath tube (cm). d is the decline coefficient of the elongation rate of sheath, per unit of exposed sheath length ($°Cd^{-1}$) .

The criterion for the optimization was to minimize the sum of squared differences between the simulated and observed length of the exposed part of sheaths at the moment when sheath is mature simultaneously for all phytomers. The rate of the length of E_n increases with time equal to the sum of the elongation rate of sheath and internode of the phytomer in question. Initial sheath elongation rate at collar emergence was set to fitted linear elongation rate for each individual rank, and the length of E_n at collar emergence was set to 0.1 cm. Average internode elongation rate was used. This average elongation rate of internode is calculated based on the duration between collar emergence and the time when sheath is mature and internode length increase during this period according to the data set based on multi-phase models for the growth of each organ, as parameterized by Andrieu *et al.* (2006). The value was subsequently fine-tuned such that modelled final sheath length approximated observed values at normal density .

Table S1. Simulation scenarios for exploring the cause of reduction of final length of blade at high ranks

Scenarios	Standard settings	Replacing $r_{B,n}$ [1]	Replacing e [2]
S1	√		
S2	√	√	
S3	√	√	√

[1]For simulations at high density condition, replacing the $r_{B,n}$ fitted for normal density by the $r_{B,n}$ fitted for high density for ranks beyond 8.
[2]Replacing the single value of maximum elongation e by the linear elongation rate estimated for each rank ($k_{B,n}$) in Andrieu *et al.* (2006).

Fig. S1. Visualization of the extension of blades (dark green), sheaths (light green) and internodes (orange) for individual maize phytomers 1 to 15 (from left to right) at (a) 238 °Cd, (b) 443 °Cd, and (c) 612 °Cd. Maize phytomers have been represented next to instead of on top of each other to clearly show the individual organs and their sizes.

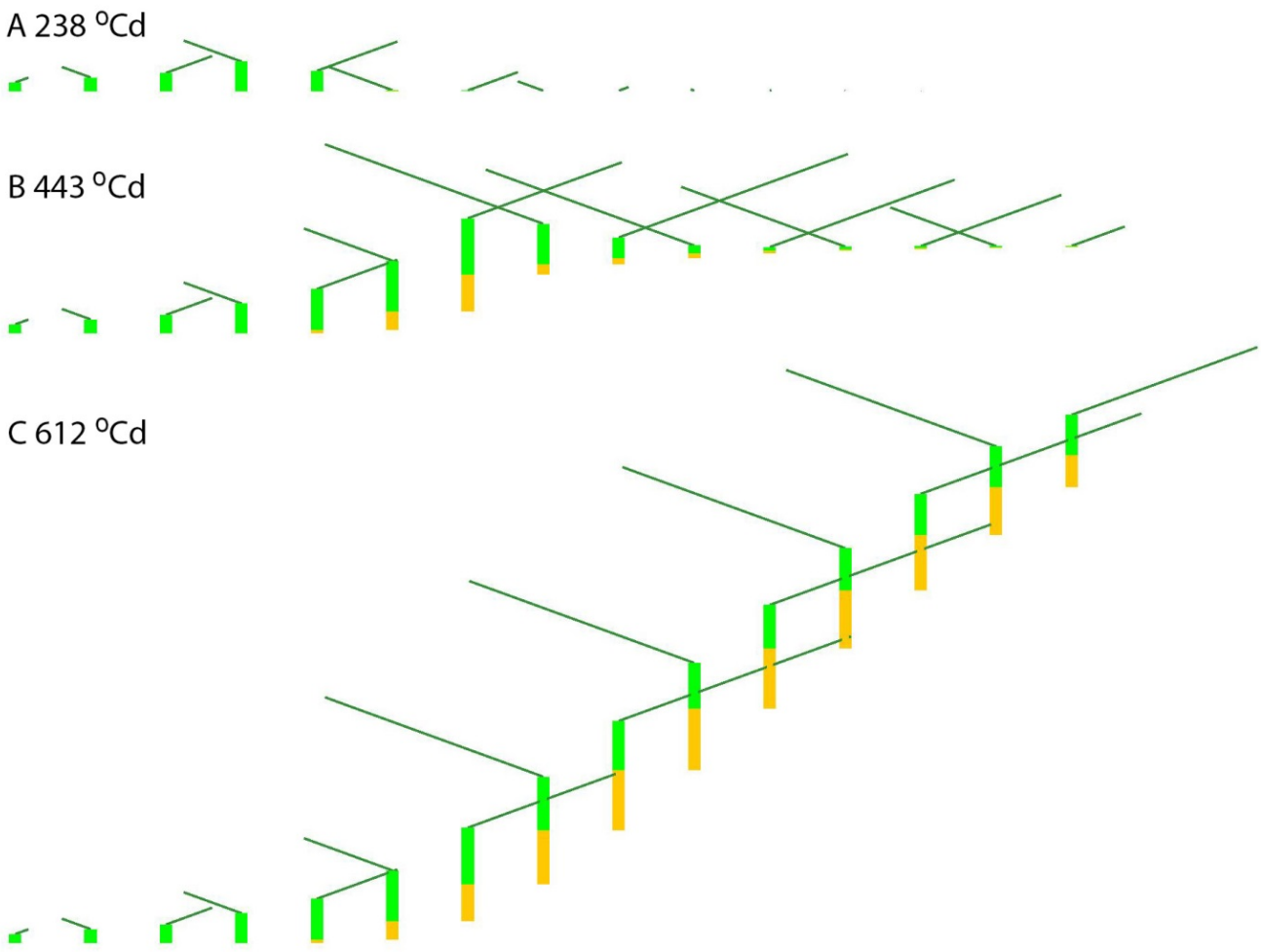

Fig. S2. The ratio of final internode length of rank *n* and final sheath length of rank *n*-1 versus the relative rank defined as the current rank divided by the final leaf number. Data are for maize cv. 'Déa' at normal density in 1996 (squares) and in 2000 (open circles), and at high density in 2000 (filled circles), and cv. 'Nobilis' at normal density in 1998 (triangles) and in 2000 (diamonds). The line is the fitted curve of the quadratic function that we used.

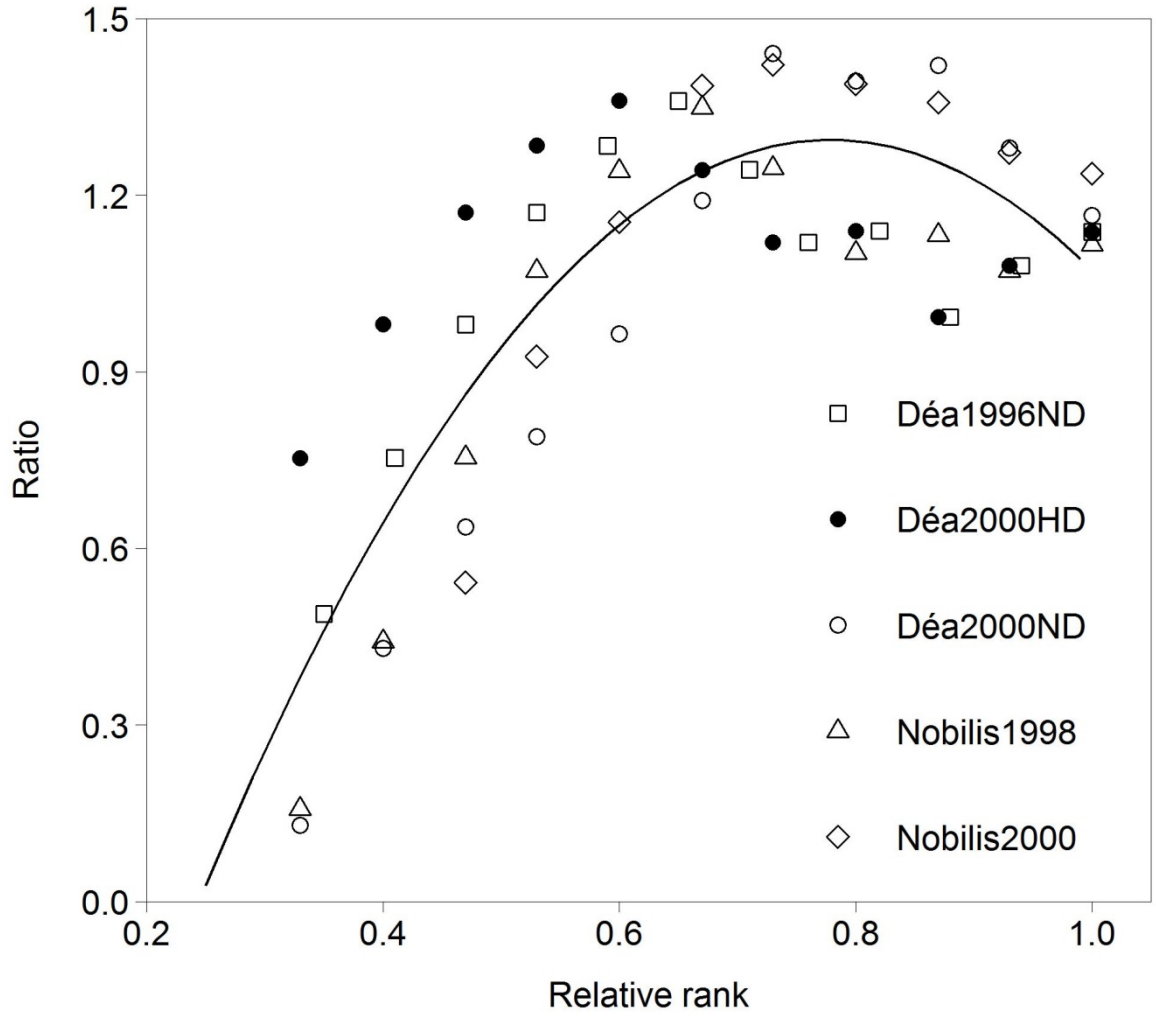

Fig. S3. Dynamics of length growth of sheath 1 (circles), 2 (triangles) and 3 (squares) for normal density (A) and high density (B) against thermal time. Symbols are measurements from maize cv. 'Déa' in 2000, and lines are fitted by equation Eq. S3 (below) including an exponential phase and a linear phase (Hillier et al., 2005).

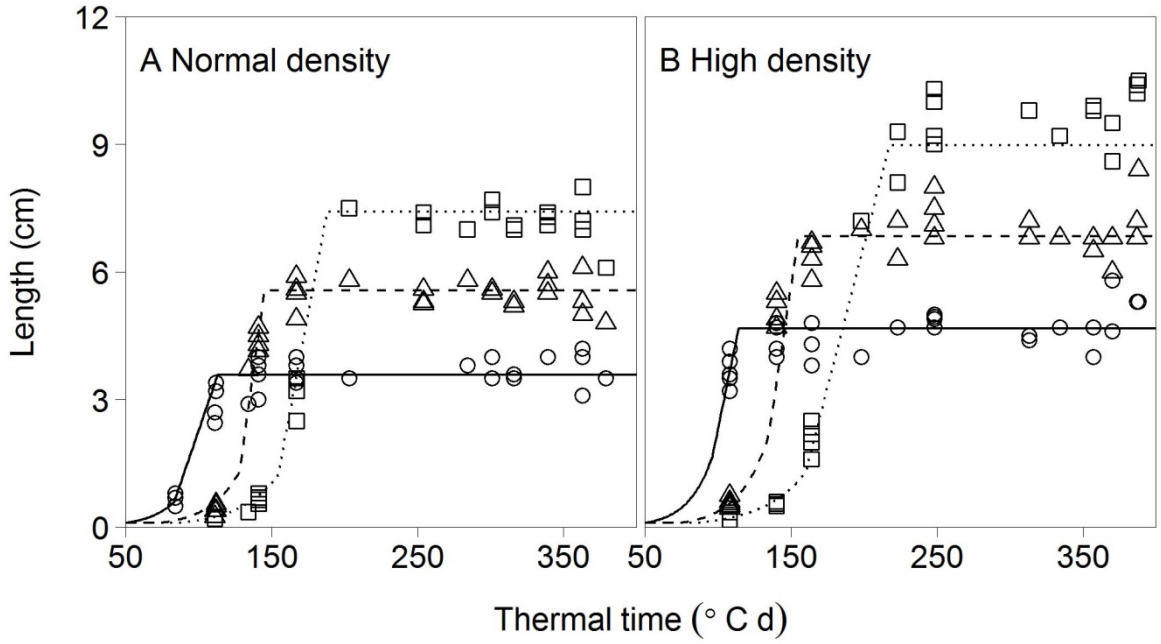

Fitting was conducted using non-linear least squares optimization was conducted in R, using function optim() with appropriate starting values. The fitting procedure was repeated using different sets of starting values to check robustness of the fitted parameter values.

$$S_{n,t} = \begin{cases} S_0 * e^{R_1(t-T_0)} & T_0 < t \le T_1 \\ S_{n,T1} + R_2(t-T_1) & T_1 < t \le T_2 \\ S_{n,\,fin} & t > T_2 \end{cases} \qquad \text{(Eq. S3)}$$

Where $S_{n,t}$ is the length of sheath n at time t. T_0 (°Cd) is the point in thermal time at which the model begins, which corresponds to the moment when $S = S_0$. $S_{n,T1}$ is the sheath length at the end of the exponential phase (T_1). $S_{n,fin}$ is the final length of sheath n that was reached at the end of linear phase (T_2). R_1 is the relative elongation rate at the exponential phase. R_2 is the linear elongation rate at the linear phase.

Fig. S4. Relationship derived from maize cultivar ‘Dea’ between blade age at sheath initiation (y-axis) and blade age at tip emergence (x-axis). Blade age was counted from the moment of initiation and expressed in °Cd. Data represent normal density (squares) and high density (circles). Open symbols represent sheaths that initiated before tassel initiation, and filled symbols represent sheaths that initiated after tassel initiation.

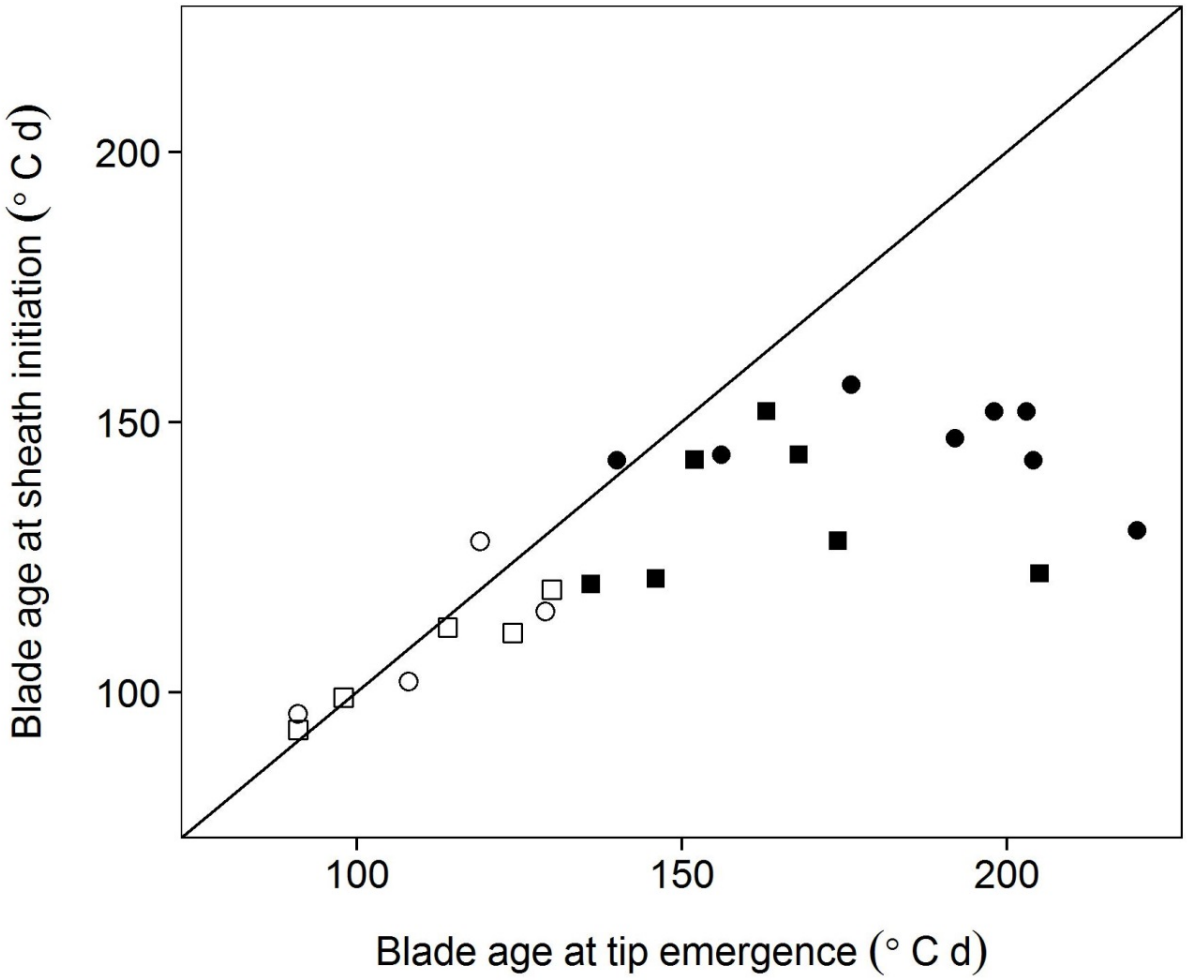

Fig. S5. (A) Final blade length of ranks 4-15 at normal density in scenarios S1 (solid line), S3 (dotted line); (B) Final blade length at ranks 4-15 at high density in scenarios S1 (solid line), S2 (dashed line), S3 (dotted line). See Table S1 for a description of the scenarios. Symbols are measurements on maize 'Déa' in 2000.

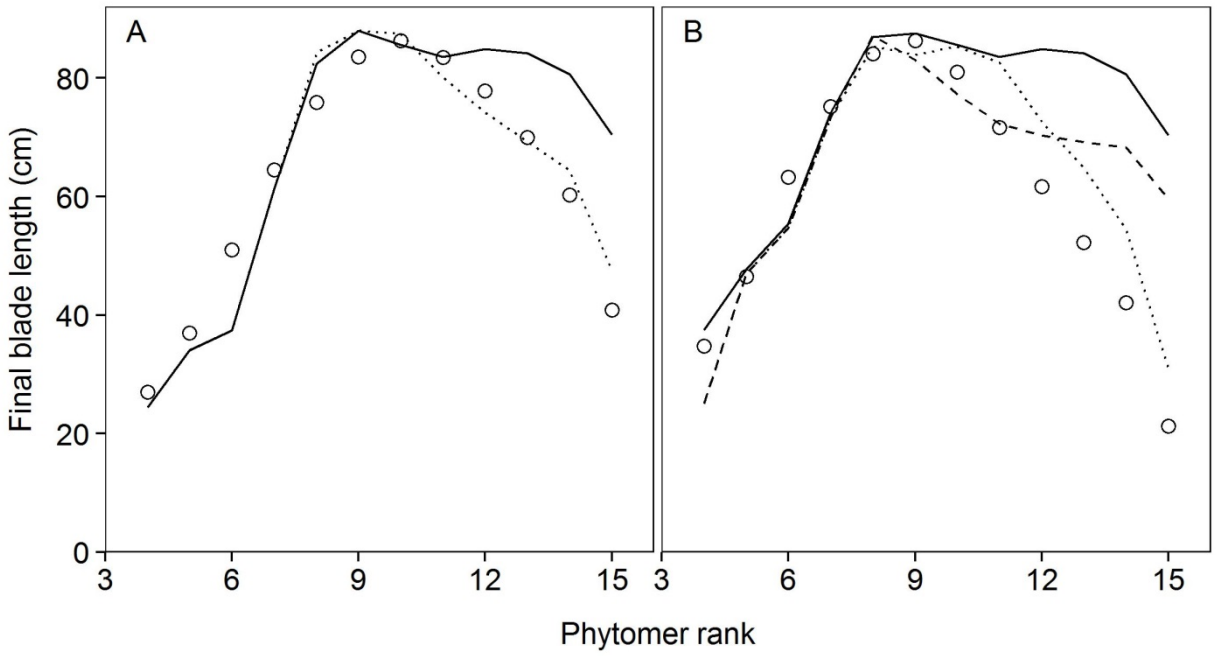

Fig. S6. The depth of sheath tube over time at normal density maize 'Déa' in 2000. Vertical dotted lines indicate the collar emergence time of ranks 4-15. The depth of sheath tube in this graph is calculated as the length of the sheath *n* which has the highest collar at the plant at that time minus the length of internode *n*+1. The gradual decrease of the depth of sheath tube represents the extension of internode *n*+1. The rapid drops represent represents the length of internode *n*+2 at the moment of collar emergence *n*+1, which become the highest collar at that moment. Note the depth of sheath tube for all un-emerged leaf tips and collars are different even at the same time because of the difference in the position of each leaf. The high rank leaves was elevated by the internode below it. Thus when sheath *n* has the highest collar at the plant, the depth of sheath tube for leaf *n*+*x* is $S_n - \sum_{n+1}^{n+x} I_n$.

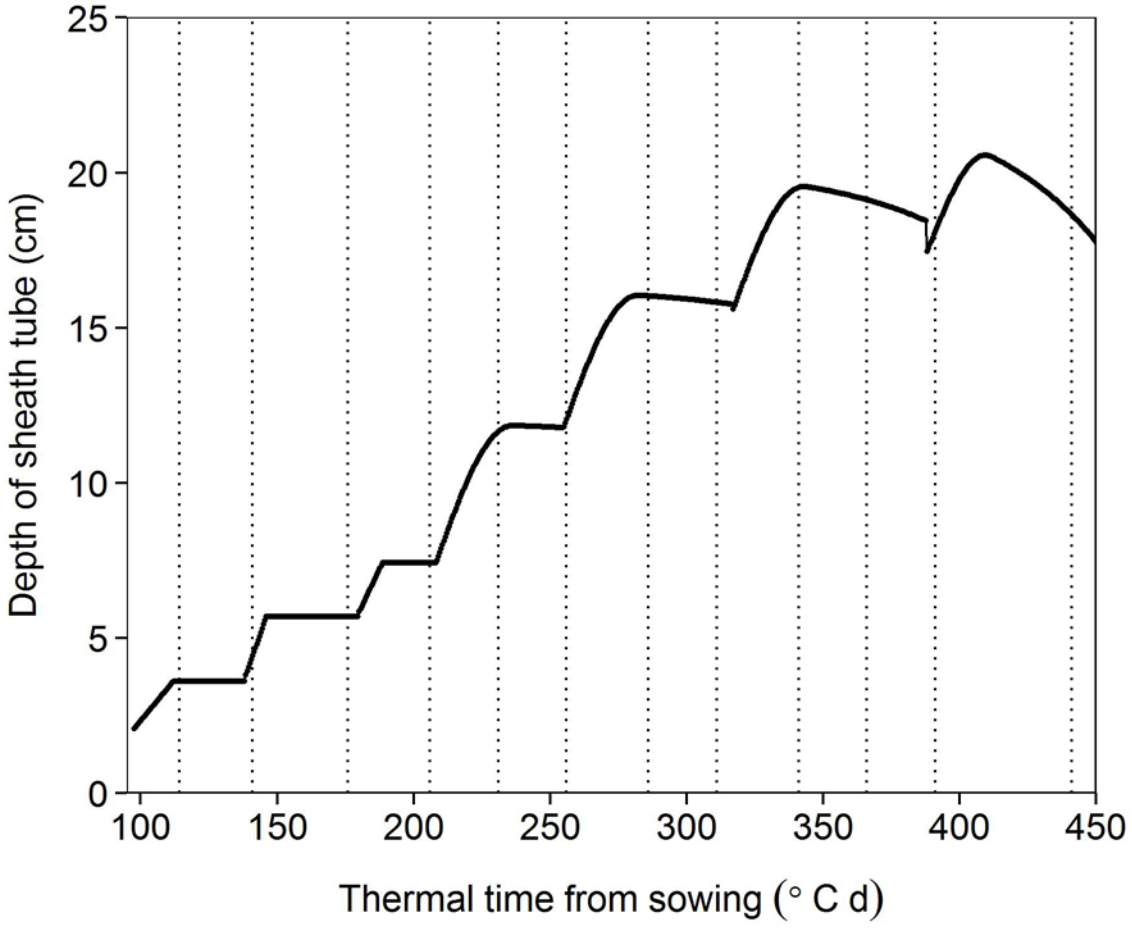

Fig. S7. Simulation results of only input the length dynamics of the first sheath. (A) Tip emergence (circles and solid line) and collar emergence (triangles and dashed line), and (B) final length of blade (circles and solid line), sheath (triangles and dashed line) and internode (squares and dotted line) versus phytomer rank. Symbols are measurements from normal density maize 'Déa' in 2000, and lines are simulations with only input the dynamics of first sheath length, collar emergence of first rank and tip emergence of first three ranks.

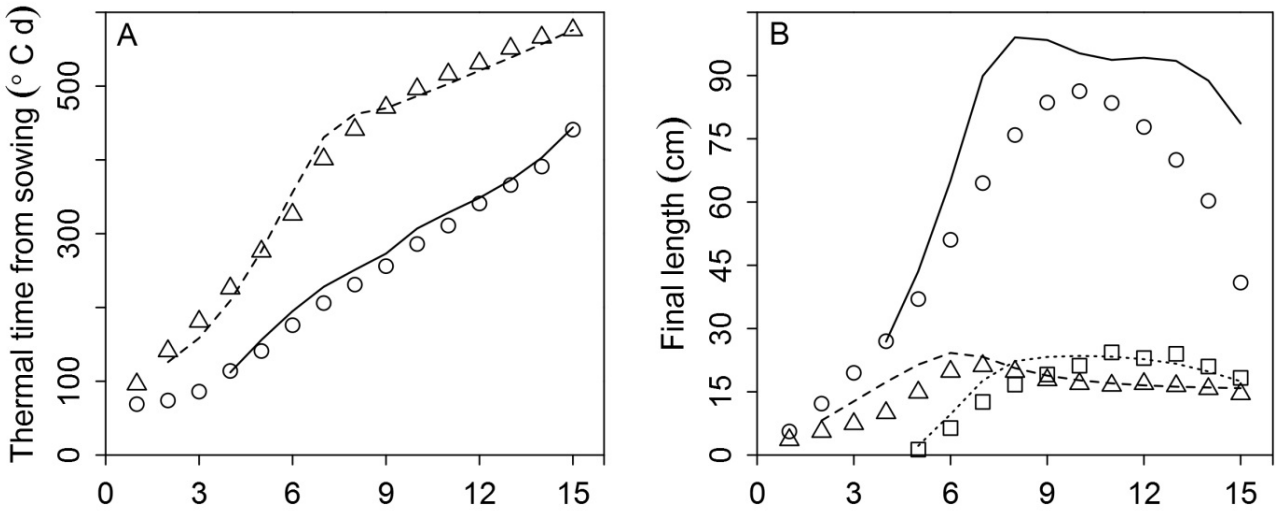

Note with the current parameter settings for all sheaths, the model overestimated the sheath length of rank 2 and 3. This overestimation propagate to blade and sheath of the following phytomers.

Literature cited for justification of coordination rules used in the model

Andrieu B, Hillier J, Birch C. 2006. Onset of sheath extension and duration of lamina extension are major determinants of the response of maize lamina length to plant density. *Annals of Botany* **98**(5): 1005-1016.

Begg JE, Wright MJ. 1962. Growth and development of leaves from intercalary meristems in phalaris arundinacea l. **194**(4833): 1097-1098.

Casey IA, Brereton AJ, Laidlaw AS, McGilloway DA. 1999. Effects of sheath tube length on leaf development in perennial ryegrass (lolium perenne l.). *Annals of Applied Biology* **134**(2): 251-257.

Davidson J, Milthorpe F. 1966. Leaf growth in dactylis glomerate following defoliation. *Annals of Botany* **30**(2): 173-184.

Fournier C, Andrieu B. 2000a. Dynamics of the elongation of internodes in maize (zea mays l.): Analysis of phases of elongation and their relationships to phytomer development. *Annals of Botany* **86**(3): 551-563.

Fournier C, Andrieu B. 2000b. Dynamics of the elongation of internodes in maize (zea mays l.): Effects of shade treatment on elongation patterns. *Annals of Botany* **86**(6): 1127-1134.

Hillier J, Makowski D, Andrieu B. 2005. Maximum likelihood inference and bootstrap methods for plant organ growth via multi-phase kinetic models and their application to maize. *Annals of Botany* **96**(1): 137-148.

Kiesselbach TA. 1999. *The structure and reproduction of corn*: Cold spring harbor laboratory press.

Parent B, Conejero G, Tardieu F. 2009. Spatial and temporal analysis of non-steady elongation of rice leaves. *Plant, Cell & Environment* **32**(11): 1561-1572.

Paysant-Leroux C. 1998. *Mise en place de la longueur et de la largeur des feuilles de maïs. Etablissement d'un modèle de développement à l'échelle de la plante pour deux génotypes.*, Université de Pau et des Pays de l'Adour Pau, France.

R Core Team 2012. R: A language and environment for statistical computing.In. Vienna, Austria: R Foundation for Statistical Computing.

Schnyder H, Seo S, Rademacher IF, Kühbauch W. 1990. Spatial distribution of growth rates and of epidermal cell lengths in the elongation zone during leaf development in *lolium perenne l. Planta* **181**(3): 423-431.

Sharman BC. 1942. Developmental anatomy of the shoot of zea mays l. *Annals of Botany* **6**(2): 245-282.

Siemer EG, Leng ER, Bonnett OT. 1969. Timing and correlation of major developmental events in maize, zea mays l. *Agronomy Journal* **61**(1): 14-17.

Skinner RH, Nelson CJ. 1994. Epidermal cell division and the coordination of leaf and tiller development. *Annals of Botany* **74**(1): 9-16.

Wilson RE, Laidlaw AS. 1985. The role of the sheath tube in the development of expanding leaves in perennial ryegrass. *Annals of Applied Biology* **106**(2): 385-391.